CalDAG-GEFI Down-Regulation in the Striatum as a Neuroprotective Change in Huntington's Disease

Jill R. Crittenden[1, 2, 3], Denise E. Dunn[4], Farhan I. Merali[1, 2], Ben Woodman[5], Michael Yim[1, 2], Anna E. Borkowska[1, 2, 3], Matthew P. Frosch[6], Gillian P. Bates[5], David E. Housman[3], Donald C. Lo[4] & Ann M. Graybiel[1, 2, *]

[1]McGovern Institute for Brain Research, MIT, 43 Vassar Street, Building 46-6133, Cambridge, MA, USA.

[2]Department of Brain and Cognitive Sciences, MIT, 43 Vassar Street, Building 46-6133, Cambridge, MA, USA.

[3]Koch Institute for Integrative Cancer Research, MIT, 77 Massachusetts Avenue, Building E17-110, Cambridge, MA, USA.

[4]Center for Drug Discovery and Department of Neurobiology, Duke University Medical Center, 4321 Medical Park Drive, Duke University Medical Center, Durham, NC, USA.

[5]Department of Medical and Molecular Genetics, King's College London School of Medicine, 8th Floor Tower Wing, Guy's Hospital, London SE1 9RT, UK.

[6]C.S. Kubik Laboratory for Neuropathology, Massachusetts General Hospital, Boston, MA, USA.

* To whom correspondence should be addressed. TEL: 617-253-5785; FAX: 617-253-1599; Email: graybiel@mit.edu

ABSTRACT

Huntingtin protein (Htt) is ubiquitously expressed, yet Huntington's disease (HD), a fatal neurologic disorder produced by expansion of an Htt polyglutamine tract, is characterized by neurodegeneration that occurs primarily in the striatum and cerebral cortex. Such discrepancies between sites of expression and pathology occur in multiple neurodegenerative disorders associated with expanded polyglutamine tracts. One possible reason is that disease-modifying factors are tissue-specific. Here we show that the striatum-enriched protein, CalDAG-GEFI, is severely down-regulated in the striatum of mouse HD models and is down-regulated in HD individuals. In the R6/2 transgenic mouse model of HD, striatal neurons with the largest aggregates of mutant Htt have the lowest levels of CalDAG-GEFI. In a brain-slice explant model of HD, knock-down of CalDAG-GEFI expression rescues striatal neurons from pathology induced by transfection of polyglutamine-expanded Htt exon 1. These findings suggest that the striking down-regulation of CalDAG-GEFI in HD could be a protective mechanism that mitigates Htt-induced degeneration.

INTRODUCTION

The symptoms of HD include uncontrollable choreic movements and mood disturbances that progress until death, which typically occurs ten to twenty years after disease onset (1-2). There is an inverse correlation between the age of symptom onset and the length of a polyglutamine tract encoded by a CAG repeat within exon 1 of the *IT15* gene (3-5). With disease progression, there is increasing loss of particular neuronal subtypes in the striatum and cerebral cortex of HD patients and, to a lesser degree, in other brain regions as well (6). It is unclear why, even within the severely affected striatum, subsets of neurons are differentially sensitive to mutant Htt. Transcriptional profiling studies of striatal and cortical postmortem tissue from HD patients and mouse models of HD have, however, identified candidate susceptibility factors as well as potentially protective, compensatory changes in gene expression (7-10).

One of the most significant transcriptional changes indicated by microarray studies of HD patients and animal models is the down-regulation of *CalDAG-GEFI* (a.k.a. *RasGRP2*) (7-9, 11). *CalDAG-GEFI* encodes a notably striatum-enriched cytoplasmic signaling molecule that has binding sites for calcium and diacylglycerol (DAG) and nucleotide exchange factor domains that target the small G proteins, Rap1 and Rap2 (12-14). We have shown that signaling from CalDAG-GEFI to Rap-family GTPases in platelets and neutrophils is critical for integrin-dependent cell adhesion and vesicle release *in vivo* (13, 15-16). In the brain, we have shown that *CalDAG-GEFI* is predominantly expressed in medium spiny projection neurons of the striatum (12, 17) and in a subset of cortical neurons, cell types that are selectively destroyed in HD. *CalDAG-GEFI* is not expressed at high levels by striatal interneurons, which are

relatively spared in HD (18-19). Further, *CalDAG-GEFI* is differentially enriched in the matrix compartment of the striatum, relative to its levels in the striosomal compartment (12). This differential distribution is significant in light of evidence that, within the HD striatum, predominant neurodegeneration can occur in either one of these two striatal compartments (20-23) and is correlated with distinct symptom profiles (22).

Given this evidence, we examined CalDAG-GEFI protein expression in HD and HD mouse models and directly tested in an *in vitro* HD striatal assay whether CalDAG-GEFI expression could influence striatal pathology. We found that CalDAG-GEFI was down-regulated in postmortem striatal samples from intermediate- and late-stage HD patients, as well as in the striatum of both the R6/1 and R6/2 mouse models of HD. In the R6/2 mouse striatum, we tracked the timing of CalDAG-GEFI down-regulation and found it to correspond to the timing of disease progression. Unexpectedly, we found that the degree of down-regulation was strongly correlated with the size of the polyglutamine-expanded Htt aggregates in striatal neurons. We therefore examined the possibility that reduced CalDAG-GEFI might mitigate cellular vulnerability to mutant Htt. We found that knock-down of CalDAG-GEFI expression protected striatal neurons from the severe pathology induced by polyglutamine-expanded Htt exon 1 in an organotypic striatal slice culture. These findings raise the clinically interesting possibility that reduced expression of CalDAG-GEFI in HD occurs as a neuroprotective mechanism to limit Htt-induced neuropathology.

RESULTS

CalDAG-GEFI is down-regulated in Huntington's Disease

To test whether the expression of CalDAG-GEFI protein is disrupted in HD, we obtained postmortem tissue from the striatum of three patients with Huntington's disease, one with intermediate-stage HD (Grade II-III) and two with late-stage HD (Grade IV) (6), and from sex-matched control brains that did not show striatal pathology. Western blot analysis showed that CalDAG-GEFI immunoreactivity was diminished in the striatal samples from all three HD brains, relative to those from the control brains (Fig. 1A). Based on comparison with a standard curve generated from 2X to 0.25X serial dilutions of the pooled control samples, this corresponded to 34 ± 12% (mean ± SEM) less CalDAG-GEFI protein in the HD striatum than in controls (Fig. 1A). These results confirm and extend the finding in microarray studies of severe down-regulation of *CalDAG-GEFI* mRNA in the striatum of HD patients (8-9).

To establish an experimental model for testing the effects of CalDAG-GEFI in HD, we next tested for the loss of CalDAG-GEFI in the most widely characterized mouse model of HD, the R6/2 line (24). R6/2 mice carry a transgene encoding the first exon of human *IT15* with a CAG expansion of over 140 repeats. The onset of motor impairments occurs in these mice before 8 weeks of age, and their symptoms develop to include choreic and stereotypic movements, tremor and seizures that progress until death, at about 13 weeks of age (24). Severe shrinkage of brain neuropil occurs in the R6/2 mice, but cell death is minimal by comparison with that occurring in HD patients (24-25).

In Western blots of brain tissue lysates from 12 week-old R6/2 mice, we found that CalDAG-GEFI immunoreactivity was reduced by 49% in the striatum ($P < 0.02$) and 40% in neocortex ($P < 0.03$), relative to that measured in age-matched controls (Fig. 1B and C). By contrast, there was not a significant difference in the expression of CalDAG-GEFI in hippocampal lysates from the two genotypes ($P > 0.6$; Fig. 1D), suggesting that the down-regulation of CalDAG-GEFI is limited to specific brain regions. We tracked the development of this deficit by harvesting brain tissue from R6/2 mice and littermate controls at 4, 8 and 12 weeks of age and examining the distribution of CalDAG-GEFI protein by immunohistochemistry (Fig. 1E). The immunoreactivity appeared slightly diminished in striatal brain sections from 4 week-old R6/2 mice (Fig. 1E), a time-point at which transcriptional changes are modest (10), but phenotypic abnormalities become apparent (10, 26-28). We observed progressive loss of CalDAG-GEFI immunostaining in 8 and 12 week-old R6/2 mice (Fig. 1E), ages at which increasingly severe motor complications occur (24). We also examined CalDAG-GEFI expression in symptomatic, 9 month old R6/1 mice, which carry the same transgene as R6/2 mice, but which exhibit a slower disease progression as a result of reduced transgene expression (24). We observed severely diminished CalDAG-GEFI immunoreactivity in these late-stage mice as well (Fig. 1F). CalDAG-GEFI immunostaining was clearly matrix-predominant at each age in both the R6/1 and R6/2 mutants and the control mice (Fig. 1G and H). These findings demonstrate that, with disease progression and increasing severity of disease symptoms, CalDAG-GEFI expression is progressively lost in the striatum of R6/1 and R6/2 mice, as in the human HD striatum, and that the loss is selective for the matrix compartment of the striatum.

To examine further the tissue-specificity of CalDAG-GEFI down-regulation, we measured CalDAG-GEFI expression and function in platelets from R6/2 mice. CalDAG-GEFI is strongly expressed in platelets from normal mice and is critical for integrin-dependent platelet adhesion and aggregation (13, 29). Western blots of platelet lysates from 12 week-old R6/2 mice and age-matched controls showed no significant differences in CalDAG-GEFI expression (Supplementary Material, Fig. S1A). Furthermore, we found that platelets from 12 week-old R6/2 mice undergo normal CalDAG-GEFI-mediated aggregation (Supplementary Material, Fig. S1B). Thus, the down-regulation of CalDAG-GEFI that occurs in striatum and cortex of R6/2 mice is not a generalized effect in all cells expressing CalDAG-GEFI.

CalDAG-GEFI expression is inversely correlated with Htt aggregate size in R6/2 model mice

In R6/2 mice, we observed that a subset of striatal neurons maintained normal levels of CalDAG-GEFI immunoreactivity in their cell bodies, despite the overall down-regulation of striatal CalDAG-GEFI expression (Fig. 2A, right panel). These neurons appeared to be of the medium-sized neuronal phenotype that characterizes striatal projection neurons, which are normally enriched in CalDAG-GEFI (12, 17). Further, we found that these neurons co-expressed EGFP reporter genes that mark the expression of the striatum-enriched D1 and D2 dopamine receptors (Fig. 2B and C) (30). Thus, the scattered neurons with high levels of CalDAG-GEFI expression in the striatum of R6/2 mice appeared to be dopaminoreceptive neurons that had not undergone down-regulation of CalDAG-GEFI. Spurred by this observation, we examined the same brains

to determine which striatal neurons exhibited Htt protein aggregates, a neuropathologic hallmark of HD (31-32). Aggregates of mutant Htt are found in the nucleus and cytoplasm of neurons throughout the neocortex and, to a lesser degree, the striatum of patients with HD and R6/2 model mice (33-35). In accord with these findings, Htt-positive neuronal intranuclear inclusions were abundant in the striatum and neocortex of the 12 week-old R6/2 mice (Fig. 2D, right panel).

We found a striking correspondence between the striatal neurons that maintained CalDAG-GEFI expression and the striatal neurons that lacked Htt-positive nuclear inclusions. Figure 2D shows the results of experiments in which we detected immunoreactivity for CalDAG-GEFI with antibodies conjugated to a red fluorophore and detected Htt with antibodies conjugated to a green fluorophore. CalDAG-GEFI did not colocalize with the intranuclear Htt inclusions (Fig. 2E), indicating that the loss of CalDAG-GEFI staining in the cytoplasm was not the result of sequestration in Htt inclusions. We applied deconvolution microscopy to obtain volumetric measurements of Htt-positive nuclear inclusions in striatal neurons that had high, intermediate or low levels of CalDAG-GEFI immunostaining. Striatal neurons with low levels of CalDAG-GEFI had nuclear inclusions that were roughly three-fold larger than the nuclear inclusions in striatal neurons with high levels of CalDAG-GEFI immunostaining (Fig. 2F and G). This inverse correlation between Htt-positive inclusion volume and CalDAG-GEFI expression was highly significant ($P < 0.0001$).

Knock-down of CalDAG-GEFI expression is neuroprotective in a brain slice model of HD

To test whether changes in CalDAG-GEFI expression levels could influence the cellular pathology associated with HD, we performed CalDAG-GEFI over-expression and knock-down experiments in a rat organotypic cortico-striatal slice model of HD (36-38). A biolistic device was used to transfect these explants with exon 1 of human Htt bearing a polyglutamine expansion of 73 polyglutamines. In this system, the transfection of polyglutamine-expanded Htt exon 1 has been shown to induce progressive dendritic and cell body degeneration of medium spiny striatal neurons that can be visualized by co-transfection with yellow fluorescent protein (YFP; Fig. 3A-D) (36-38).

As in these previous studies, we observed that the number of healthy striatal neurons was reduced by ~2-fold in brain slices that were transfected with the mutant Htt construct, relative to the numbers found in the striatum of control slices transfected with YFP marker alone (Fig. 3E, $P < 0.01$). However, when we co-transfected cortico-striatal brain slices with the polyglutamine-expanded Htt exon 1 and with an siRNA that targets CalDAG-GEFI (15), the numbers of healthy striatal neurons were restored to control levels, relative to the numbers of healthy neurons in slices that were co-transfected with a control siRNA (Fig. 3E, $P < 0.01$). To ensure that the siRNA effectively knocked down rat CalDAG-GEFI, we transfected the rat striatal cell line ST14A with increasing concentrations of siRNA. We observed a dose-dependent reduction in CalDAG-GEFI protein expression, relative to cells transfected with a non-targeting control siRNA (Fig. 3F). We also confirmed that the siRNA was effective in the explant system. We co-transfected slices with YFP, siRNA and a CalDAG-GEFI-tdTomato fusion construct and then evaluated the tdTomato fluorescence intensity of medium spiny striatal cells that were co-tranfected with CalDAG-GEFI siRNA vs. control siRNA (Supplementary

Material, Fig. S2). In the slices that were co-transfected with CalDAG-GEFI siRNA, we found that there were significantly more cells classified as dim ($P < 10^{-5}$), and significantly fewer cells classified as bright ($P < 10^{-5}$), for expression of the CalDAG-GEFI-tdTomato protein, relative to slices transfected with control siRNA. Thus, the siRNA targeting CalDAG-GEFI effectively knocked-down expression of the CalDAG-GEFI-tdTomato fusion construct in the explant system.

As a control for the effects of CalDAG-GEFI knock-down alone, we repeated these experiments, transfecting the CalDAG-GEFI siRNA without co-transfection of the mutant Htt construct. There was no change in the numbers of healthy neurons relative to treatment with the control siRNA, demonstrating that the rescue effect of the CalDAG-GEFI siRNA was specific to the presence of mutant Htt exon 1 (Fig. 3G). When we transfected YFP siRNA alone, the number of visible YFP-positive neurons visible was minimal, reflecting nearly complete knock-down of YFP protein expression and indicating that the siRNA transfection system itself was effective (Fig. 3G). Finally, we co-transfected slices with a CalDAG-GEFI over-expression construct together with the Htt construct and YFP. Whereas knock-down of CalDAG-GEFI rescued mutant Htt exon 1-induced pathology in the slice system, over-expression of CalDAG-GEFI tended to exacerbate the toxic effects of mutant Htt on the striatal neurons (Fig. 3H, $P = 0.05$).

DISCUSSION

Our findings suggest that the striatum-enriched signaling molecule, CalDAG-GEFI, may be functionally linked to neuronal degeneration in HD. CalDAG-GEFI protein levels were markedly decreased in the striatum of intermediate- and late-stage HD human brains examined and in the striatum of symptomatic R6/1 and R6/2 HD model mice. The down-regulation appeared to be tissue-specific, given that CalDAG-GEFI expression was normal in the hippocampus and in platelets from R6/2 mice with end-stage disease. This tissue-selectivity of CalDAG-GEFI down-regulation stands in contrast to the regulation of numerous other genes that show parallel dysregulation in both brain and non-nervous system tissue in R6/2 mice, as tested in brain and muscle microarray assays (10).

Scattered cells within the striatum of R6/2 mice maintained high levels of CalDAG-GEFI expression, and these cells had markedly smaller Htt-positive nuclear inclusions than did those with low CalDAG-GEFI expression. The CalDAG-GEFI-positive cells had the morphological appearance of medium-sized neurons and were dopaminoreceptive, judging from co-expression of EGFP BAC transgene reporters for either the Drd1a or the Drd2 dopamine receptors. These CalDAG-GEFI-enriched striatal neurons were presumed to be of the projection neuron phenotype, as *CalDAG-GEFI* mRNA is predominantly expressed in these neurons in wild-type animals (17) and CalDAG-GEFI protein is transported from the striatum to terminal sites in the pallidum and substantia nigra (12).

Such an inverse relationship is not the general rule for genes expressed in the striatum. It has been reported that there is no correlation between the presence of

aggregates and the down-regulation of at least three other striatum-enriched genes in the R6/2 mouse model (39).

The correlation between Htt-positive aggregate size and low CalDAG-GEFI expression demonstrated here raises as alternative possibilities that either 1) Htt aggregates, or correlated factors, inhibit CalDAG-GEFI expression, perhaps through the sequestration of transcription factors as recently shown for other striatum-enriched genes (11), or 2) CalDAG-GEFI blocks aggregate formation, perhaps through its downstream target, Rap2, which is implicated in aggresome formation (40-41) or 3) these processes work in combination. However, we did not observe obvious differences in the frequency of aggregates in striatal neurons in brain slice explants transfected with YFP and polyglutamine-expanded Htt exon 1 fused to cyan fluorescent protein (CFP) when CalDAG-GEFI expression was either knocked down or augmented (Supplementary Material, Fig. S3). Thus, our data indicate that the beneficial effects of CalDAG-GEFI knock-down in the explant assay are not related to aggregate formation. If this finding extends to striatal neurons in R6/2 mice, then aggregate formation might precede, and promote, CalDAG-GEFI down-regulation in this model. Together with our findings that CalDAG-GEFI is strongly down-regulated in the HD striatum, and that CalDAG-GEFI is lost gradually over time in the R6/2 striatum, our results suggest that in HD, striatal neurons increasingly down-regulate CalDAG-GEFI as cellular pathology progresses.

Our *in vitro* findings demonstrate that knock-down of CalDAG-GEFI expression, which mimics its down-regulation in HD and HD models, rescues striatal neurons from the neuropathology induced by polyglutamine-expanded Htt exon 1 (36-38).

Conversely, over-expression of CalDAG-GEFI in the brain slice model exacerbated the neuronal pathology associated with expression of polyglutamine-expanded Htt in this assay. Whereas knock-down of CalDAG-GEFI provided complete rescue from the pathology that was measured in this assay system, overexpression of CalDAG-GEFI had only a modest effect. This contrast likely reflects the fact that basal levels of CalDAG-GEFI are already so high in striatal neurons that overexpression has relatively little effect on CalDAG-GEFI signaling pathways. Nevertheless, this set of results concordantly support the hypothesis that down-regulation of CalDAG-GEFI is neuroprotective against neurodegenerative processes induced by polyglutamine-expanded Htt exon 1.

The mechanisms that might underlie this effect are as yet unclear, but they could involve elimination of toxic conformations of Htt or down-regulation of calcium-induced cytotoxic signaling. The calcium binding motifs in CalDAG-GEFI suggest that the protein might be highly sensitive to excitotoxic signaling, suggested to occur in HD (42-43). Experimentally-induced strong excitation of the neocortex elevates intracellular calcium and activates the extracellular-regulated kinases, ERK1/2, in striatal neurons (44-46). In heterologous cell culture systems, CalDAG-GEFI regulates ERK (12, 47). These findings raise the possibility that compensatory down-regulation of CalDAG-GEFI might influence ERK signaling in the HD models. However, the role of ERK1/2 activation in the pathogenesis of HD remains unclear. Activated ERK1/2 levels are elevated in the striatum of R6/2 mice, despite an apparent reduction in downstream ERK1/2 signaling (48). In cell culture, it has been shown that potentiation of the ERK1/2 signaling cascade diminishes cell-death caused by expanded Htt expression (44, 49). ERK1/2 signaling is

also implicated in another hyperkinetic movement condition, L-DOPA-induced dyskinesia. ERK1/2 activity is elevated in models of L-DOPA-induced dyskinesia and blockade of this activity alleviates the abnormal movements. We previously have found, in a rat model of L-DOPA-induced dyskinesia, that the matrix-enriched CalDAG-GEFI is down-regulated, whereas the striosome-enriched paralog, CalDAG-GEFII, is upregulated (50). We suggested that the opposing dysregulation of these two ERK1/2 regulators could contribute to the imbalance in striosome:matrix activity observed in models of L-DOPA-induced dyskinesia. Similarly, the down-regulation of CalDAG-GEFI in HD would be expected to have compartment-specific effects. However, to our knowledge, the dysregulation of ERK1/2 activity in relation to these compartments has not been examined in HD models. What is known is that either the striosome or the matrix compartment can be differentially affected in HD brains examined post-mortem, suggesting that compartmentalized gene expression is likely to be important in the etiology or expression of the disorder.

The working hypothesis prompted by these findings is that as the expression of CalDAG-GEFI falls in HD, a neuroprotective effect of CalDAG-GEFI down-regulation, possibly through ERK1/2 regulation and/or calcium signaling, would thus increase. Several other calcium-responsive signal transduction molecules are down-regulated in HD (51), but whether their down-regulation is neuroprotective has not been demonstrated.

Our findings extend evidence that changes in calcium-related signaling could be significant in HD (43), and further suggest that the effects of this signaling could have an impact on CalDAG-GEFI-dependent mechanisms such as cell adhesion, vesicle release

and Ras/Rap/ERK signaling in the striatum. As CalDAG-GEFI is normally expressed predominantly in projection neurons in the matrix compartment of the striatum, aberrant calcium signaling in matrix-based pathways could be a major feature of the disease process even before massive loss of tissue. In the brains of HD patients studied postmortem, both matrix-predominant patterns of cell loss and striosome-predominant patterns of cell loss have been observed, with each being correlated to individual symptom profiles (20-23). Our findings suggest that CalDAG-GEFI-related signaling pathways could contribute to these differential pathologies by virtue of their predominant expression in the matrix compartment, particularly related to sensory-motor functions of the striatum and cortico-basal ganglia pathways.

Within the striatum, the striatal interneurons that express low levels of CalDAG-GEFI are initially spared in HD, relative to the severe neurodegeneration that occurs in the CalDAG-GEFI-enriched projection neurons. Along with neurodegeneration of the striatum, select areas of the neocortex undergo thinning in the earliest, pre-symptomatic stages of HD (52-53); although CalDAG-GEFI is expressed in subsets of cortical neurons in rodents (17), we have not determined whether these cell types correspond to the complex pattern of cortical degeneration observed in human HD. Nevertheless, the pattern of relative loss in the striatum could indicate that high levels of cytoplasmic CalDAG-GEFI are correlated with selective vulnerability to Htt-induced toxicity. This possibility is supported by our observation that CalDAG-GEFI over-expression in organotypic brain slices exacerbates the degeneration of striatal neurons transfected with polyglutamine-expanded Htt exon 1. Critically, co-transfection with an siRNA knock-down construct for CalDAG-GEFI rescued neuronal pathology in the brain slice

model. Thus, our findings are consistent with the hypothesis that the expression of CalDAG-GEFI in medium spiny striatal neurons and in a subset of cortical neurons confers differential vulnerability of these cell types to neuropathology associated with mutant Htt.

CalDAG-GEFI is one of the most heavily down-regulated transcripts identified in microarray screens for transcriptome changes in HD and models of HD (7-9, 11). Our findings raise the possibility that this down-regulation could represent an endogenous, homeostatic mechanism countering neuronal dysfunction in the striatum in HD. If so, early regulation of CalDAG-GEFI expression could represent a novel therapeutic strategy for early intervention.

MATERIALS AND METHODS

Animal husbandry

Mice and rats were maintained under a standard light/dark cycle with free access to food and water. Procedures for the mouse studies were in strict accordance with the MIT Committee on Animal Care, accredited by AAALAC (USA), and with Home Office (UK) regulations. All procedures used for the rats were in strict accordance with Duke Institutional Animal Care and Use Committee guidelines.

Mouse brain immunolabeling

Brains were obtained from R6/1 and R6/2 female mice and age-matched controls (generated by breeding R6/1 or R6/2 males to [CBA/Ca x C57BL/6/J] F1 females

[B6CBAF1/OlaHsd, Harlan Olac, Bichester, UK]) from the laboratory of Dr. Gillian Bates. Mice were deeply anesthetized prior to transcardial perfusion with buffered 4% paraformaldehyde. Brains were stored and shipped to MIT in a cryoprotectant buffer, and 24 μm-thick frozen transverse sections through the striatum were cut on a sliding microtome. Sections were processed for immunohistochemistry with rabbit polyclonal anti-CalDAG-GEFI antiserum #3752 (13) and anti-rabbit antibody coupled to biotin for ABC amplification (Vector Laboratories). Sections from the R6/2 and R6/1 and control mice were processed in parallel by an individual blinded to genotype.

Brain sections from R6/2 mice that carried a Drd1a-EGFP or Drd2-EGFP BAC transgene were processed for immunofluorescence with anti-CalDAG-GEFI antiserum #3752 plus anti-EGFP antiserum (Abcam). Sections were subsequently incubated with anti-rabbit coupled to ALEXA594 antiserum plus anti-goat coupled to ALEXA488 antiserum (Invitrogen Corp.). Sections were mounted and coverslipped with Vectashield media (Vector Laboratories) and imaged on an Olympus BX61 fluorescent microscope with an Olympus DP70 digital camera.

Human tissue isolation

Frozen brain tissue was provided by the Neuropathology Core of the Massachusetts Alzheimer Disease Research Center and was prepared as described by Vonsattel and coworkers (54). The control samples were from 45, 82 and 92 year old males with no remarkable brain pathology, the HD case samples were from 48, 59 and 72 year old males who were judged to have moderate to severe degeneration of the striatum and scattered ubiquitin-positive intranuclear inclusions.

Immunoblotting

To prepare striatal tissue from mice, brains were removed from deeply anesthetized R6/2 male mice and age-matched sibling controls and striatal tissue was immediately dissected and frozen. Platelets were isolated by collecting blood into serum-separation tubes, spinning serum for 10 min at 3,000 X g and freezing platelet pellets on dry ice. Samples from the human caudate nucleus and putamen were dissected from frozen sections. Tissue was homogenized in ice-cold modified RIPA buffer (50 mM Tris pH 8.0, 150 mM NaCl, 1% Triton X-100, 0.1% sodium dodecyl sulfate, 1% NaDeoxycholate) with Complete protease inhibitor cocktail (Roche) and was centrifuged at 16,000 X g for 10 min to remove insoluble material. Supernatants were analyzed by bicinchoninic acid assays (Thermo Fisher Scientific) to determine total protein concentration. Protein (40 μg lysate per lane) was resolved by SDS-PAGE and transferred to PVDF membrane (Millipore) by electroblotting. Blots were incubated with anti-CalDAG-GEFI rabbit polyclonal antiserum #3752 (13) and anti-rabbit antibody coupled to horseradish peroxidase prior to immunodetection with Western Lightening (PerkinElmer Inc.) according to the manufacturer's instructions. Blots were subsequently incubated with anti-β-tubulin (Cell Signaling Technology) or anti-Tuj1 (Abcam Inc.) antibodies to control for protein loading. Blots were scanned (UMAX), and the pixel density and size of the immunoreactive bands was calculated with ImageJ (NIH). To normalize for background signal and protein loading, the mean pixel density of an equivalently-sized area below the immunoreactive band was subtracted from each band and the result was divided by

the mean pixel density of the normalized Tuj1 band. Normalized intensity results were averaged within genotypes for comparison.

Deconvolution microscopy

Sections through the striatum were processed as described above for immunohistochemistry except that sections were double-labeled by simultaneous incubation with rabbit anti-CalDAG-GEFI and mouse monoclonal EM48 anti-Htt antibodies (MAB5374; Chemicon International) followed by fluorescent secondary antibodies (anti-mouse coupled to ALEXA 488 and anti-rabbit coupled to ALEXA 564; Invitrogen Corp.). Sections were mounted and coverslipped with Vectashield media (Vector Laboratories).

A 100X objective on a Zeiss Axioplan 2 microscope fitted with a Hamamatsu ORCA-ER digital camera was used to obtain images from the medial striatum in two sections each from the brains of three R6/2 female mice (12 week-old). Striatal neurons were rated as having high, medium or low levels of anti-CalDAG-GEFI immunofluorescence by observation through the red channel alone to prevent biased cell-selection based on inclusion size (visible only through the green channel). Subsequently, a Z-stack of images through each neuron (Z step = 0.5 μm) was acquired on the green channel, using Openlab Improvision software. Automatic exposure normalization was followed to control for variable staining intensity among the sections. Z-series data were deconvolved using Volocity Improvision software, and volume measurements of the MAB5374-immunoreactive inclusions were calculated by Volocity.

Transfection of ST14A cells

To test siRNA efficiency, ST14A cells were grown in Dulbecco's Modified Eagle's media and fetal calf serum to 50% confluency in a 48-well tissue culture dish and transfected with CalDAG-GEFI or non-targeting siRNA (Integrated DNA Technologies) with Lipofectamine 2000 (Invitrogen) following manufacturer's instructions. Forty-eight hours later, cells were lysed in RIPA buffer with Complete protease inhibitor cocktail (Roche) in preparation for CalDAG-GEFI immunoblotting,

Cortico-striatal organotypic brain slice assay

Cortico-striatal brain slices (250 μm-thick) from Sprague-Dawley rat pups (Charles River, postnatal day 10) were cut on a vibratome. The slices were maintained in interface cultures with culture medium containing 15% heat-inactivated horse serum, 10 mM KCl, 10 mM HEPES, 100 U/ml penicillin/streptomycin, 1 mM MEM sodium pyruvate, and 1 mM L-glutamine in Neurobasal A (Invitrogen) under 5% CO_2 at 32°C. A biolistic device (Helios Gene Gun; Bio-Rad) was then used to transfect brain slices with 1.6 μm gold particles (BioRad) that can bind plasmid DNAs as previously described (55), or with surface-modified gold particles (Seashell Technology) capable of binding both plasmid DNA and siRNAs. The Htt expression plasmid used contained human *IT15* exon 1 with a 73 polyglutamine repeat subcloned into the gWIZ expression vector (Gene Therapy Systems, Inc.) and was constructed based on clones and sequences that were generous gifts of Dr. Christopher Ross (Johns Hopkins University) and the Hereditary Disease Foundation. The CalDAG-GEFI over-expression construct consisted of a full-length mouse CalDAG-GEFI cDNA subcloned into a separate gWIZ expression

plasmid. The CalDAG-GEFI-tdTomato fusion construct was generated by cloning mouse CalDAG-GEFI cDNA into the 3' end of the Living Colors tdTomato vector (Clontech). The siRNA against CalDAG-GEFI was generated by Integrated DNA Technologies with the targeting sequence 5'-AAAGCGCAAGATGTCCCTGTT-3' (15). Brain slices were co-transfected with a YFP expression construct in all cases so that medium spiny neurons could be imaged and identified by their location within the striatum and by their characteristic dendritic arborization. Medium spiny neurons exhibiting normal cell body diameters, even and continuous expression of YFP within all cell compartments, and more than two discernable primary dendrites with each more than two cell body-diameters long were scored as "healthy" (see Figure 3A).

For estimation of aggregate frequencies, a similar Htt exon 1 construct was used with the same 73 polyglutamine repeat but also included a C-terminal fusion with cyan fluorescent protein to allow direct visualization of aggregate formation. For these experiments, brain slices were fixed 24 hours after biolistic transfection in order to capture the initial phases of aggregate formation; fixation was done using 2.5% paraformaldehyde, 0.5% glutaraldehyde, and 4% sucrose in PBS. After 30 minutes, slices were washed extensively with PBS and mounted in Vectashield (Vector Labs). Cells were imaged on an Olympus BX61 fluorescent microscope with an Olympus DP70 digital camera.

SUPPLEMENTARY MATERIAL

Supplementary Material is available at *HMG* online.

ACKNOWLEDGEMENTS

We thank Dr. Elena Cattaneo for the gift of ST14A cells, Dr. Christopher Ross for *Htt* constructs and Dr. Wolfgang Bergmeier for his help with the platelet assays. We are grateful to P. Harlan, H. Hall, K. Fischer, and Zachary Crook for technical support and to Drs. Kyle Copps and Ruth Bodner for critical comments.

Conflict of Interest statement. None declared.

FUNDING

This work was supported by the National Institute of Child Health and Development [R01-HD28341 to A.M.G.]; the James and Pat Poitras Research Fund to A.M.G.; the National Institutes of Mental Health [F32-MH065815 to J.R.C.]; the Wellcome Trust to G.P.B.; the Cure Huntington's Disease Initiative, Inc. to D.C.L.; the Hereditary Disease Foundation to D.C.L. and D.E.H.; Neuropathology Cores of the Massachusetts Alzheimer Disease Research Center [P50-AG005134 to M.P.F.] and the MGH/MIT Morris Udall Center of Excellence in Parkinson disease research [P50-NS038372 to M.P.F.] .

REFERENCES

1 Bates, G. and Harper, P.S. (2002) *Huntington's Disease*. Oxford University Press, New York.

2 Harper, P.S. (2001) *Huntington's Disease*. W.B. Saunders, London.

3 The Huntington's Disease Collaborative Research Group (1993) A novel gene containing a trinucleotide repeat that is expanded and unstable on Huntington's disease chromosomes. *Cell*, **72**, 971-983.

4 Wexler, N.S., Lorimer, J., Porter, J., Gomez, F., Moskowitz, C., Shackell, E., Marder, K., Penchaszadeh, G., Roberts, S.A., Gayan, J. *et al.* (2004) Venezuelan kindreds reveal that genetic and environmental factors modulate Huntington's disease age of onset. *Proc. Natl. Acad. Sci. USA*, **101**, 3498-3503.

5 Becher, M.W., Kotzuk, J.A., Sharp, A.H., Davies, S.W., Bates, G.P., Price, D.L. and Ross, C.A. (1998) Intranuclear neuronal inclusions in Huntington's disease and dentatorubral and pallidoluysian atrophy: correlation between the density of inclusions and IT15 CAG triplet repeat length. *Neurobiol. Dis.*, **4**, 387-397.

6 Vonsattel, J.-P., Myers, R.H., Stevens, T.J., Ferrante, R.J., Bird, E.D. and Richardson, E.P., Jr. (1985) Neuropathological classification of Huntington's Disease. *J. Neuropathol. Exp. Neurol.*, **44**, 559-577.

7 Morton, A.J., Hunt, M.J., Hodges, A.K., Lewis, P.D., Redfern, A.J., Dunnett, S.B. and Jones, L. (2005) A combination drug therapy improves cognition and reverses gene expression changes in a mouse model of Huntington's disease. *Eur. J. Neurosci.*, **21**, 855-870.

8 Desplats, P.A., Kass, K.E., Gilmartin, T., Stanwood, G.D., Woodward, E.L., Head, S.R., Sutcliffe, J.G. and Thomas, E.A. (2006) Selective deficits in the expression of striatal-enriched mRNAs in Huntington's disease. *J. Neurochem.*, **96**, 743-757.

9 Kuhn, A., Goldstein, D.R., Hodges, A., Strand, A.D., Sengstag, T., Kooperberg, C., Becanovic, K., Pouladi, M.A., Sathasivam, K., Cha, J.H. *et al.* (2007) Mutant huntingtin's effects on striatal gene expression in mice recapitulate changes observed in human Huntington's disease brain and do not differ with mutant huntingtin length or wild-type huntingtin dosage. *Hum. Mol. Genet.*, **16**, 1845-1861.

10 Luthi-Carter, R., Hanson, S.A., Strand, A.D., Bergstrom, D.A., Chun, W., Peters, N.L., Woods, A.M., Chan, E.Y., Kooperberg, C., Krainc, D. *et al.* (2002) Dysregulation of gene expression in the R6/2 model of polyglutamine disease: parallel changes in muscle and brain. *Hum. Mol. Genet.*, **11**, 1911-1926.

11 Desplats, P.A., Lambert, J.R. and Thomas, E.A. (2008) Functional roles for the striatal-enriched transcription factor, Bcl11b, in the control of striatal gene expression and transcriptional dysregulation in Huntington's disease. *Neurobiol. Dis.*, **31**, 298-308.

12 Kawasaki, H., Springett, G.M., Toki, S., Canales, J.J., Harlan, P., Blumenstiel, J.P., Chen, E.J., Bany, I.A., Mochizuki, N., Ashbacher, A. *et al.* (1998) A Rap guanine nucleotide exchange factor enriched highly in the basal ganglia. *Proc. Natl. Acad. Sci. USA*, **95**, 13278-13283.

13 Crittenden, J.R., Bergmeier, W., Zhang, Y., Piffath, C.L., Liang, Y., Wagner, D.D., Housman, D.E. and Graybiel, A.M. (2004) CalDAG-GEFI integrates signaling for platelet aggregation and thrombus formation. *Nature Med.*, **10**, 982-986.

14 Ohba, Y., Mochizuki, N., Matsuo, K., Yamashita, S., Nakaya, M., Hashimoto, Y., Hamaguchi, M., Kurata, T., Nagashima, K. and Matsuda, M. (2000) Rap2 as a

slowly responding molecular switch in the Rap1 signaling cascade. *Mol. Cell. Biol.*, **20**, 6074-6083.

15 Ghandour, H., Cullere, X., Alvarez, A., Luscinskas, F.W. and Mayadas, T.N. (2007) Essential role for Rap1 GTPase and its guanine exchange factor CalDAG-GEFI in LFA-1 but not VLA-4 integrin mediated human T-cell adhesion. *Blood*, **110**, 3682-3690.

16 Bergmeier, W., Goerge, T., Wang, H.-W., Crittenden, J.R., Baldwin, A.C.W., Cifuni, S.M., Housman, D.E., Graybiel, A.M. and Wagner, D.D. (2007) Mice lacking the signaling molecule CalDAG-GEFI represent a model for leukocyte adhesion deficiency type III. *J. Clin. Invest.*, **117**, 1699-1707.

17 Toki, S., Kawasaki, H., Tashiro, N., Housman, D.E. and Graybiel, A.M. (2001) Guanine nucleotide exchange factors CalDAG-GEFI and CalDAG-GEFII are colocalized in striatal projection neurons. *J. Comp. Neurol.*, **437**, 398-407.

18 Dawbarn, D., De Quidt, M.E. and Emson, P.C. (1985) Survival of basal ganglia neuropeptide Y-somatostatin neurons in Huntington's disease. *Brain Res.*, **340**, 251-260.

19 Ferrante, R.J., Kowall, N.W., Beal, M.F., Richardson, E.P., Jr., Bird, E.D. and Martin, J.B. (1985) Selective sparing of a class of striatal neurons in Huntington's disease. *Science*, **230**, 561-563.

20 Hedreen, J.C. and Folstein, S.E. (1995) Early loss of neostriatal striosome neurons in Huntington's disease. *J. Neuropathol. Exp. Neurol.*, **54**, 105-120.

21 Reiner, A., Albin, R.L., Anderson, K.D., D'Amato, C.J., Penney, J.B. and Young, A.B. (1988) Differential loss of striatal projection neurons in Huntington disease. *Proc. Natl. Acad. Sci. USA*, **85**, 5733-5737.

22 Tippett, L.J., Waldvogel, H.J., Thomas, S.J., Hogg, V.M., van Roon-Mom, W., Synek, B.J., Graybiel, A.M. and Faull, R.L.M. (2007) Striosomes and mood dysfunction in Huntington's disease. *Brain*, **130**, 206-221.

23 Ferrante, R.J., Kowall, N.W., Beal, M.F., Martin, J.B., Bird, E.D. and Richardson, E.P., Jr. (1987) Morphologic and histochemical characteristics of a spared subset of striatal neurons in Huntington's disease. *J. Neuropathol. Exp. Neurol.*, **46**, 12-27.

24 Mangiarini, L., Sathasivam, K., Seller, M., Cozens, B., Harper, A., Heterington, C., Lawton, M., Trottier, Y., Lehrach, H., Davies, S.W. *et al.* (1996) Exon 1 of the HD gene with an expanded CAG repeat is sufficient to cause a progressive neurological phenotype in transgenic mice. *Cell*, **87**, 493-506.

25 Stack, E.C., Kubilus, J.K., Smith, K., Cormier, K., Del Signore, S.J., Guelin, E., Ryu, H., Hersch, S.M. and Ferrante, R.J. (2005) Chronology of behavioral symptoms and neuropathological sequela in R6/2 Huntington's disease transgenic mice. *J. Comp. Neurol.*, **490**, 354-370.

26 Cepeda, C., Hurst, R.S., Calvert, C.R., Hernandez-Echeagaray, E., Nguyen, O.K., Jocoy, E., Christian, L.J., Ariano, M.A. and Levine, M.S. (2003) Transient and progressive electrophysiological alterations in the corticostriatal pathway in a mouse model of Huntington's disease. *J. Neurosci.*, **23**, 961-969.

27 Lione, L.A., Carter, R.J., Hunt, M.J., Bates, G.P., Morton, A.J. and Dunnett, S.B. (1999) Selective discrimination learning impairments in mice expressing the human Huntington's disease mutation. *J. Neurosci.*, **19**, 10428-10437.

28 Murphy, K.P., Carter, R.J., Lione, L.A., Mangiarini, L., Mahal, A., Bates, G.P., Dunnett, S.B. and Morton, A.J. (2000) Abnormal synaptic plasticity and impaired spatial cognition in mice transgenic for exon 1 of the human Huntington's disease mutation. *J. Neurosci.*, **20**, 5115-5123.

29 Eto, K., Murphy, R., Kerrigan, S.W., Bertoni, A., Stuhlmann, H., Nakano, T., Leavitt, A.D. and Shattil, S.J. (2002) Megakaryocytes derived from embryonic stem cells implicate CalDAG-GEFI in integrin signaling. *Proc. Natl. Acad. Sci. USA*, **99**, 12819-12824.

30 Gong, S., Zheng, C., Doughty, M.L., Losos, K., Didkovsky, N., Schambra, U.B., Nowak, N.J., Joyner, A., Leblanc, G., Hatten, M.E. *et al.* (2003) A gene expression atlas of the central nervous system based on bacterial artificial chromosomes. *Nature*, **425**, 917-925.

31 Davies, S.W., Beardsall, K., Turmaine, M., DiFiglia, M., Aronin, N. and Bates, G.P. (1998) Are neuronal intranuclear inclusions the common neuropathology of triplet-repeat disorders with polyglutamine-repeat expansions? *Lancet*, **351**, 131-133.

32 La Spada, A.R. and Taylor, J.P. (2003) Polyglutamines placed into context. *Neuron*, **38**, 681-684.

33 DiFiglia, M., Sapp, E., Chase, K.O., Davies, S.W., Bates, G.P., Vonsattel, J.P. and Aronin, N. (1997) Aggregation of huntingtin in neuronal intranuclear inclusions and dystrophic neurites in brain. *Science*, **277**, 1990-1993.

34 Davies, S.W., Turmaine, M., Cozens, B.A., DiFiglia, M., Sharp, A.H., Ross, C.A., Scherzinger, E., Wanker, E.E., Magniarini, L. and Bates, G.P. (1997) Formation of neuronal intranuclear inclusions underlies the neurological dysfunction in mice transgenic for the HD mutation. *Cell*, **90**, 537-548.

35 Li, H., Li, S.H., Cheng, A.L., Mangiarini, L., Bates, G.P. and Li, X.J. (1999) Ultrastructural localization and progressive formation of neuropil aggregates in Huntington's disease transgenic mice. *Hum. Mol. Genet.*, **8**, 1227-1236.

36 Khoshnan, A., Ko, J., Watkin, E.E., Paige, L.A., Reinhart, P.H. and Patterson, P.H. (2004) Activation of the IkappaB kinase complex and nuclear factor-kappaB contributes to mutant huntingtin neurotoxicity. *J. Neurosci.*, **24**, 7999-8008.

37 Varma, H., Voisine, C., DeMarco, C.T., Cattaneo, E., Lo, D.C., Hart, A.C. and Stockwell, B.R. (2007) Selective inhibitors of death in mutant huntingtin cells. *Nat. Chem. Biol.*, **3**, 99-100.

38 Southwell, A.L., Khoshnan, A., Dunn, D.E., Bugg, C.W., Lo, D.C. and Patterson, P.H. (2008) Intrabodies binding the proline-rich domains of mutant huntingtin increase its turnover and reduce neurotoxicity. *J. Neurosci.*, **28**, 9013-9020.

39 Sadri-Vakili, G., Menon, A.S., Farrell, L.A., Keller-McGandy, C.E., Cantuti-Castelvetri, I., Standaert, D.G., Augood, S.J., Yohrling, G.J. and Cha, J.H. (2006) Huntingtin inclusions do not down-regulate specific genes in the R6/2 Huntington's disease mouse. *Eur. J. Neurosci.*, **23**, 3171-3175.

40 Ravikumar, B., Duden, R. and Rubinsztein, D.C. (2002) Aggregate-prone proteins with polyglutamine and polyalanine expansions are degraded by autophagy. *Hum. Mol. Genet.*, **11**, 1107-1117.

41 Williams, A., Sarkar, S., Cuddon, P., Ttofi, E.K., Saiki, S., Siddiqi, F.H., Jahreiss, L., Fleming, A., Pask, D., Goldsmith, P. *et al.* (2008) Novel targets for Huntington's disease in an mTOR-independent autophagy pathway. *Nat. Chem. Biol.*, **4**, 295-305.

42 Fan, M.M. and Raymond, L.A. (2007) N-methyl-D-aspartate (NMDA) receptor function and excitotoxicity in Huntington's disease. *Prog. Neurobiol.*, **81**, 272-293.

43 Bezprozvanny, I. and Hayden, M.R. (2004) Deranged neuronal calcium signaling and Huntington disease. *Biochem. Biophys. Res. Commun.*, **322**, 1310-1317.

44 Apostol, B.L., Illes, K., Pallos, J., Bodai, L., Wu, J., Strand, A., Schweitzer, E.S., Olson, J.M., Kazantsev, A., Marsh, J.L. *et al.* (2006) Mutant huntingtin alters MAPK signaling pathways in PC12 and striatal cells: ERK1/2 protects against mutant huntingtin-associated toxicity. *Hum. Mol. Genet.*, **15**, 273-285.

45 Lievens, J.C., Woodman, B., Mahal, A. and Bates, G.P. (2002) Abnormal phosphorylation of synapsin I predicts a neuronal transmission impairment in the R6/2 Huntington's disease transgenic mice. *Mol. Cell. Neurosci.*, **20**, 638-648.

46 Sgambato, V., Pages, C., Rogard, M., Besson, M.J. and Caboche, J. (1998) Extracellular signal-regulated kinase (ERK) controls immediate early gene induction on corticostriatal stimulation. *J. Neurosci.*, **18**, 8814-8825.

47 Guo, F., Kumahara, E. and Saffen, D. (2001) A CalDAG-GEFI/Rap1/B-Raf cassette couples M(1) muscarinic acetylcholine receptors to the activation of ERK1/2. *J. Biol. Chem.*, **276**, 25568-25581.

48 Roze, E., Betuing, S., Deyts, C., Marcon, E., Brami-Cherrier, K., Pages, C., Humbert, S., Merienne, K. and Caboche, J. (2008) Mitogen- and stress-activated protein kinase-1 deficiency is involved in expanded-huntingtin-induced transcriptional dysregulation and striatal death. *FASEB J*, **22**, 1083-1093.

49 Varma, H., Cheng, R., Voisine, C., Hart, A.C. and Stockwell, B.R. (2007) Inhibitors of metabolism rescue cell death in Huntington's disease models. *Proc. Natl. Acad. Sci. USA*, **104**, 14525-14530.

50 Crittenden, J.R., Cantuti-Castelvetri, I., Saka, E., Keller-McGandy, C.E., Hernandez, L.F., Kett, L.R., Young, A.B., Standaert, D. and Graybiel, A.M. (2009) Dysregulation of CalDAG-GEFI and CalDAG-GEFII predicts the severity of motor side-effects induced by anti-parkinsonian therapy. *Proc. Natl. Acad. Sci. USA*, **106**, 2892-2896.

51 Luthi-Carter, R., Strand, A., Peters, N.L., Solano, S.M., Hollingsworth, Z.R., Menon, A.S., Frey, A.S., Spektor, B.S., Penney, E.B., Schilling, G. *et al.* (2000) Decreased expression of striatal signaling genes in a mouse model of Huntington's disease. *Hum. Mol. Genet.*, **9**, 1259-1271.

52 Rosas, H.D., Hevelone, N.D., Zaleta, A.K., Greve, D.N., Salat, D.H. and Fischl, B. (2005) Regional cortical thinning in preclinical Huntington disease and its relationship to cognition. *Neurology*, **65**, 745-747.

53 Rosas, H.D., Tuch, D.S., Hevelone, N.D., Zaleta, A.K., Vangel, M., Hersch, S.M. and Salat, D.H. (2006) Diffusion tensor imaging in presymptomatic and early Huntington's disease: Selective white matter pathology and its relationship to clinical measures. *Mov. Disord.*, **21**, 1317-1325.

54 Vonsattel, J.P., Aizawa, H., Ge, P., DiFiglia, M., McKee, A.C., MacDonald, M., Gusella, J.F., Landwehrmeyer, G.B., Bird, E.D., Richardson, E.P., Jr. *et al.* (1995) An improved approach to prepare human brains for research. *J. Neuropathol. Exp. Neurol.*, **54**, 42-56.

55 Yacoubian, T.A. and Lo, D.C. (2000) Truncated and full-length TrkB receptors regulate distinct modes of dendritic growth. *Nat. Neurosci.*, **3**, 342-349.

Legends to Figures

Figure 1. CalDAG-GEFI is down-regulated in Huntington's disease. (**A**) Western blot of lysates from the striatum illustrating reduced CalDAG-GEFI immunoreactivity in three individuals with Huntington's disease (HD), relative to three control individuals. HD1 and HD2 samples were from cases with Grade IV HD and HD3 sample was from an indiviidual with Grade II-III HD. Striatal lysates from wildtype (WT) and CalDAG-GEFI knockout (KO) mice were processed in parallel to demonstrate antibody specificity (right-most two lanes of lower blot). The relative immunoreactivity in HD vs. control samples (bar graph) was calculated from a standard curve generated by serial dilution of the pooled control samples in the blot shown at top. Anti-Tuj1 bands show controls for protein loading. Data are representative of those in three experiments. (**B-D**) Western blot of lysates from striatum (**B**), neocortex (**C**) and hippocampus (**D**) from three 12 week old R6/2 mice with polyglutamine repeat lengths between 192 and 194, compared to blots from age-matched sibling controls. Reduced CalDAG-GEFI immunoreactivity is apparent in striatum and neocortex, but not hippocampus, of R6/2 mice. Anti-Tuj1 bands are shown as controls for protein loading. Bar graphs of average normalized immunoreactivity for controls and R6/2 samples are shown to the right of each blot; $*P < 0.05$. **(E)** Transverse sections from the brains of R6/2 (polyglutamine repeat lengths between 197 and 204) and control mice immunostained for CalDAG-GEFI. CalDAG-GEFI immunostaining, relative to that in controls, gradually diminished with increasing age (4, 8 and 12 weeks of age). The 12 week old R6/2 mice exhibited severe depletion of CalDAG-GEFI, especially medially. Images are representative of

immunostaining observed in 4 individual R6/2 mice of each age, compared to 4 age-matched controls. Scale bar, 1 mm. (**F**) Transverse sections from the brains of symptomatic R6/1 and control mice demonstrating down-regulation of CalDAG-GEFI immunostaining. (**G, H**) High-magnification photomicrographs illustrating CalDAG-GEFI immunostained matrix tissue surrounding a striosome (dotted outline). Scale bar, 0.1 mm. (**G**) A 12 week-old control (left) and R6/2 mutant (right). (**H**) A 9 month-old control (left) and R6/1 mutant (right).

Figure 2. CalDAG-GEFI down-regulation is correlated with Htt aggregate size in striatal neurons of R6/2 mice. (A) Immunostaining for CalDAG-GEFI in medium-sized neurons (examples at arrows) in the striatum of control (left) and 12 week-old R6/2 mutant (right), illustrating abundant CalDAG-GEFI-positive medium-sized neurons in control striatum and sharply diminished numbers of CalDAG-GEFI-positive neurons in R6/2 striatum. Scale bar indicates 100 μm. Inset on right shows magnified image of the CalDAG-GEFI immunostained neuron indicated by an arrow in R6/2 striatum. Scale bar, 50 μm. **(B, C)** Immunofluorescence for EGFP (green, left panels) and CalDAG-GEFI (red, middle panels) in 12 week-old R6/2 mice that carried a BAC transgene for the D1 dopamine receptor **(B)** or the D2 dopamine receptor **(C).** Arrows indicate cells with high levels of CalDAG-GEFI and co-expression of EGFP. Scale bars indicate 50 μm. **(D)** Double immunofluorescence for CalDAG-GEFI (red) and Htt (green) in the dorsolateral striatum and overlying neocortex of control (left) and R6/2 (right) mice. Neurons that retained CalDAG-GEFI expression in R6/2 mice exhibited reduced incidence and/or size of Htt-positive nuclear inclusions (green). Scale bar, 100 μm. **(E)** No colocalization

of CalDAG-GEFI and Htt was observed, as demonstrated by single-channel imaging of CalDAG-GEFI immunoreactivity in the cell soma (left) and Htt immunoreactivity in a neighboring aggregate (right) of the the neuron indicated in **D**. Scale bar, 50 μm. (**F**) Estimated inclusion size in 143 striatal neurons from 12 week-old R6/2 mice. Samples included 50 cells with low, 34 cells with intermediate and 59 cells with high CalDAG-GEFI immunostaining. Inclusion size and immunodetectable CalDAG-GEFI levels were inversely related ($P < 0.0001$ by Kendall correlation test). All groups were significantly different ($P < 0.01$ by Tukey's post-hoc comparison) following one-way ANOVA ($F(2, 144) = 91.15$, $P < 0.0001$). Bars show means ± SEM. (**G**) Size distribution of all inclusions that were included in the bar graph in **F**.

Figure 3. CalDAG-GEFI knock-down rescues neuropathology induced by polyglutamine-expanded Htt exon 1 in cortico-striatal brain slice explants. (A-D) Visual assessment of healthy versus unhealthy medium spiny striatal neurons in striatal organotypic brain slices. **(A)** A YFP-transfected striatal neuron, illustrating YFP-positive dendrites and a rounded cell body. **(B-D)** Examples of neurons with increasing degrees of dendritic dystrophy and loss, from slices co-transfected with polyglutamine-expanded Htt exon 1 and YFP. Scale bar, 50 μm. **(E)** Slices co-transfected with polyglutamine-expanded Htt exon 1 and YFP (light blue bars) showed about half the number of healthy striatal neurons found in slices transfected with YFP alone (dark blue bars). Transfection with a siRNA against CalDAG-GEFI rescued neuronal health of neurons co-transfected with mutant Htt exon 1 (pink bars). Data are shown for three independent experiments, with 5-20 brain slices for each bar, with corresponding SEMs. *$P < 0.01$ for within experiment comparisons of all three conditions by Dunnett's post hoc

comparison, following one-way ANOVA. **(F)** Western blots of lysates from ST14A rat striatal cells showed that transfection with CalDAG-GEFI siRNA dose-dependently knocks-down CalDAG-GEFI expression. Anti-Tuj1 bands show controls for protein loading. **(G)** Transfection of CalDAG-GEFI siRNA without concomitant transfection of mutant Htt does not increase numbers of healthy striatal neurons, relative to those in slices treated with control siRNA. YFP siRNA co-transfection leads to almost complete loss of YFP-positive neurons, demonstrating the efficiency of siRNA transfection. **(H)** Cortico-striatal brain slices co-transfected with mutant Htt exon 1 and a CalDAG-GEFI cDNA construct showed further decreases in numbers of healthy striatal neurons (red bars), relative to transfection with polyglutamine-expanded Htt exon 1. The decreases appeared proportional to the amount of CalDAG-GEFI cDNA loaded (1:1 vs. 3:1 CalDAG-GEFI:YFP DNA by mass). For the 3:1 condition, ***P* = 0.05 by Dunnett's post hoc comparison following ANOVA. Data shown were pooled from *n* = 11-12 brain slices for each bar; means ± SEM are shown. Data are representative of two independent experiments.

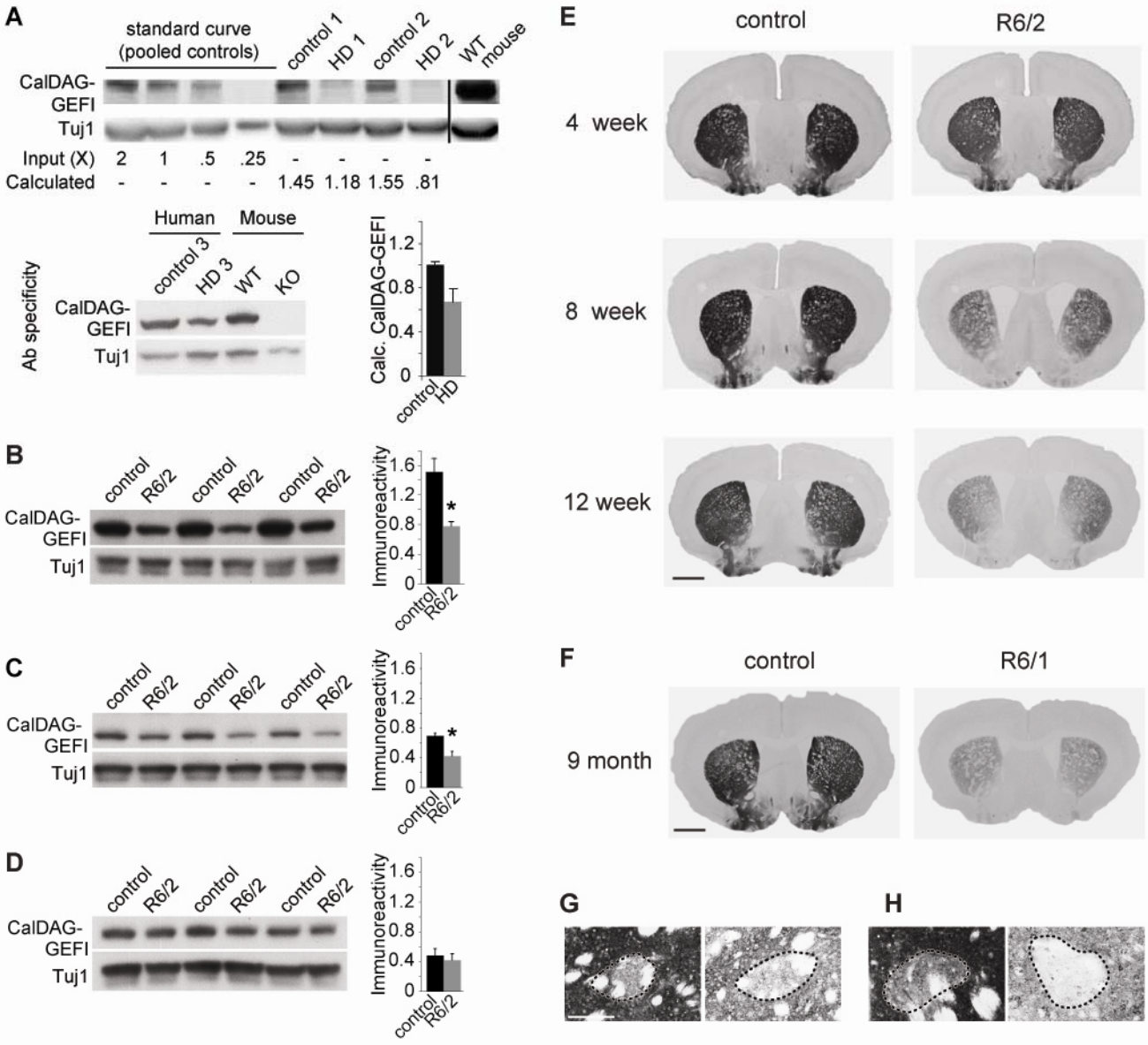

Figure 1. CalDAG-GEFI is down-regulated in Huntington's disease. (**A**) Western blot of lysates from the striatum illustrating reduced CalDAG-GEFI immunoreactivity in three individuals with Huntington's disease (HD), relative to three control individuals. HD1 and HD2 samples were from cases with Grade IV HD and HD3 sample was from an indiviidual with Grade II-III HD. Striatal lysates from wildtype (WT) and CalDAG-GEFI knockout (KO) mice were processed in parallel to demonstrate antibody specificity (right-most two lanes of lower blot). The relative immunoreactivity in HD vs. control samples (bar graph) was calculated from a standard curve generated by serial dilution of the pooled control samples in the blot shown at top. Anti-Tuj1 bands show controls for protein loading. Data are representative of those in three experiments. (**B-D**) Western blot of lysates from striatum (**B**), neocortex (**C**) and hippocampus (**D**) from three 12 week old R6/2 mice with polyglutamine repeat lengths between 192 and 194, compared to blots from age-matched sibling controls. Reduced CalDAG-GEFI immunoreactivity is apparent in striatum and neocortex, but not hippocampus, of R6/2 mice. Anti-Tuj1 bands are shown as controls for protein loading. Bar graphs of average normalized immunoreactivity for controls and R6/2 samples are shown to the right of each blot; **P* < 0.05. **(E)** Transverse sections from the brains of R6/2 (polyglutamine repeat lengths between 197 and 204) and control mice immunostained for CalDAG-GEFI. CalDAG-GEFI immunostaining, relative to that in controls, gradually diminished with increasing age (4, 8 and 12 weeks of age). The 12 week old R6/2 mice exhibited severe depletion of CalDAG-GEFI, especially medially. Images are representative of immunostaining observed in 4 individual R6/2 mice of each age, compared to 4 age-matched controls. Scale bar, 1 mm. (**F**) Transverse sections from the brains of symptomatic R6/1 and control mice demonstrating down-regulation of CalDAG-GEFI immunostaining. (**G, H**) High-magnification photomicrographs illustrating CalDAG-GEFI immunostained matrix tissue surrounding a striosome (dotted outline). Scale bar, 0.1 mm. (**G**) A 12 week-old control (left) and R6/2 mutant (right). (**H**) A 9 month-old control (left) and R6/1 mutant (right).

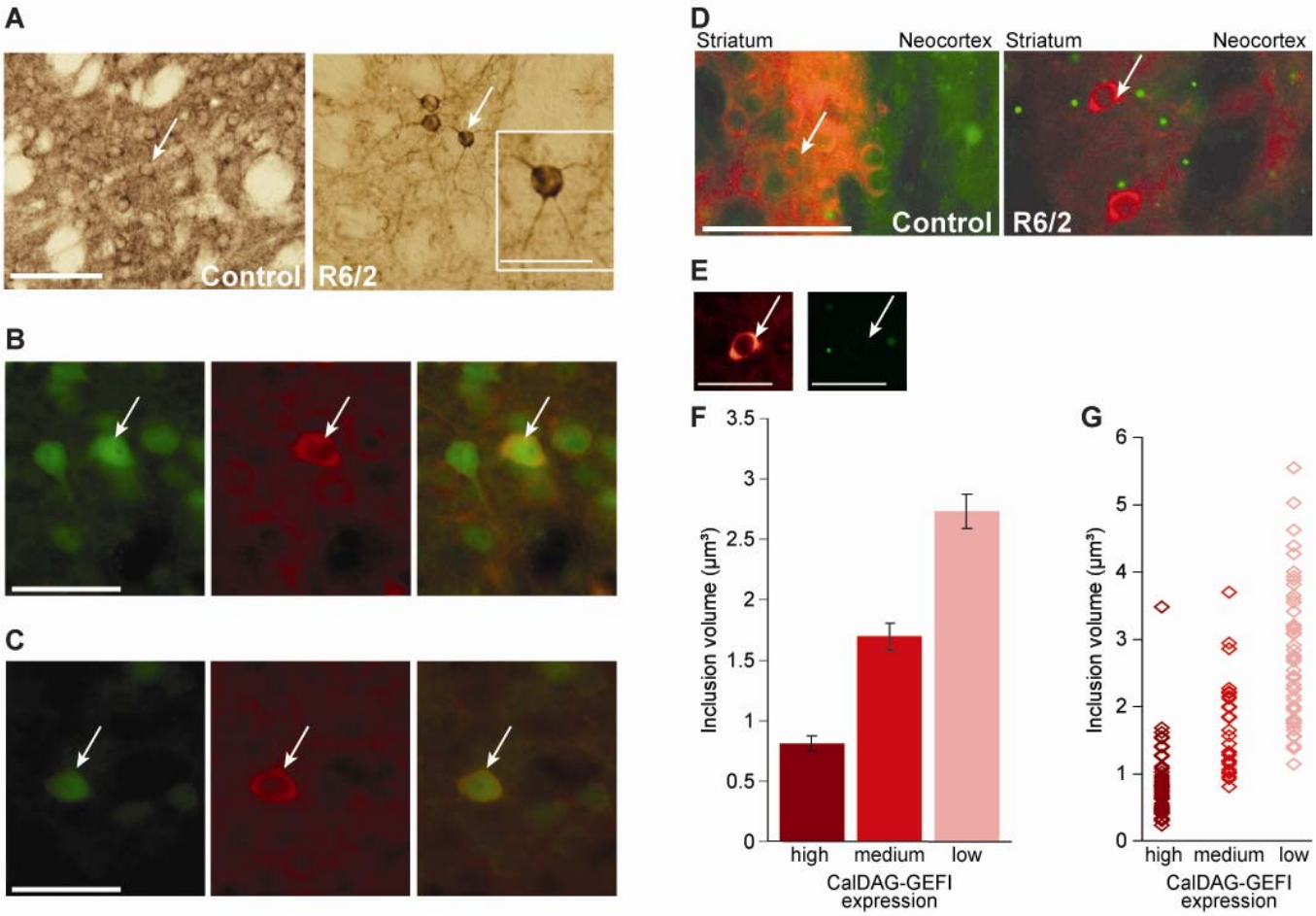

Figure 2. CalDAG-GEFI down-regulation is correlated with Htt aggregate size in striatal neurons of R6/2 mice. (A) Immunostaining for CalDAG-GEFI in medium-sized neurons (examples at arrows) in the striatum of control (left) and 12 week-old R6/2 mutant (right), illustrating abundant CalDAG-GEFI-positive medium-sized neurons in control striatum and sharply diminished numbers of CalDAG-GEFI-positive neurons in R6/2 striatum. Scale bar indicates 100 µm. Inset on right shows magnified image of the CalDAG-GEFI immunostained neuron indicated by an arrow in R6/2 striatum. Scale bar, 50 µm. **(B, C)** Immunofluorescence for EGFP (green, left panels) and CalDAG-GEFI (red, middle panels) in 12 week-old R6/2 mice that carried a BAC transgene for the D1 dopamine receptor **(B)** or the D2 dopamine receptor **(C).** Arrows indicate cells with high levels of CalDAG-GEFI and co-expression of EGFP. Scale bars indicate 50 µm. **(D)** Double immunofluorescence for CalDAG-GEFI (red) and Htt (green) in the dorsolateral striatum and overlying neocortex of control (left) and R6/2 (right) mice. Neurons that retained CalDAG-GEFI expression in R6/2 mice exhibited reduced incidence and/or size of Htt-positive nuclear inclusions (green). Scale bar, 100 µm. **(E)** No colocalization of CalDAG-GEFI and Htt was observed, as demonstrated by single-channel imaging of CalDAG-GEFI immunoreactivity in the cell soma (left) and Htt immunoreactivity in a neighboring aggregate (right) of the the neuron indicated in **D**. Scale bar, 50 µm. (**F**) Estimated inclusion size in 143 striatal neurons from 12 week-old R6/2 mice. Samples included 50 cells with low, 34 cells with intermediate and 59 cells with high CalDAG-GEFI immunostaining. Inclusion size and immunodetectable CalDAG-GEFI levels were inversely related ($P < 0.0001$ by Kendall correlation test). All groups were significantly different ($P < 0.01$ by Tukey's post-hoc comparison) following one-way ANOVA ($F(2, 144) = 91.15$, $P < 0.0001$). Bars show means ± SEM. (**G**) Size distribution of all inclusions that were included in the bar graph in **F**.

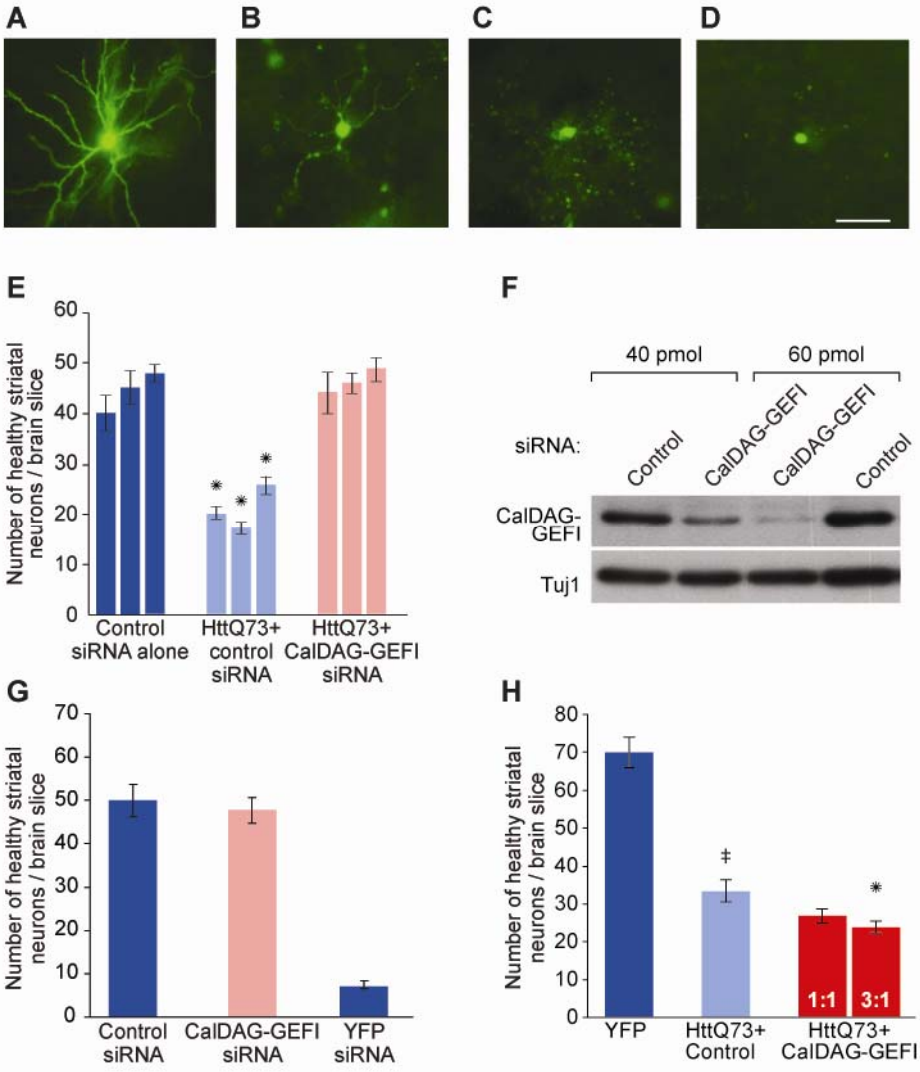

Figure 3. CalDAG-GEFI knock-down rescues neuropathology induced by polyglutamine-expanded Htt exon 1 in cortico-striatal brain slice explants. (A-D) Visual assessment of healthy versus unhealthy medium spiny striatal neurons in striatal organotypic brain slices. **(A)** A YFP-transfected striatal neuron, illustrating YFP-positive dendrites and a rounded cell body. **(B-D)** Examples of neurons with increasing degrees of dendritic dystrophy and loss, from slices co-transfected with polyglutamine-expanded Htt exon 1 and YFP. Scale bar, 50 µm. **(E)** Slices co-transfected with polyglutamine-expanded Htt exon 1 and YFP (light blue bars) showed about half the number of healthy striatal neurons found in slices transfected with YFP alone (dark blue bars). Transfection with a siRNA against CalDAG-GEFI rescued neuronal health of neurons co-transfected with mutant Htt exon 1 (pink bars). Data are shown for three independent experiments, with 5-20 brain slices for each bar, with corresponding SEMs. **P* < 0.01 for within experiment comparisons of all three conditions by Dunnett's post hoc comparison, following one-way ANOVA. **(F)** Western blots of lysates from ST14A rat striatal cells showed that transfection with CalDAG-GEFI siRNA dose-dependently knocks-down CalDAG-GEFI expression. Anti-Tuj1 bands show controls for protein loading. **(G)** Transfection of CalDAG-GEFI siRNA without concomitant transfection of mutant Htt does not increase numbers of healthy striatal neurons, relative to those in slices treated with control siRNA. YFP siRNA co-transfection leads to almost complete loss of YFP-positive neurons, demonstrating the efficiency of siRNA transfection. **(H)** Cortico-striatal brain slices co-transfected with mutant Htt exon 1 and a CalDAG-GEFI cDNA construct showed further decreases in numbers of healthy striatal neurons (red bars), relative to transfection with polyglutamine-expanded Htt exon 1. The decreases appeared proportional to the amount of CalDAG-GEFI cDNA loaded (1:1 vs. 3:1 CalDAG-GEFI:YFP DNA by mass). For the 3:1 condition, *****P* = 0.05 by Dunnett's post hoc comparison following ANOVA. Data shown were pooled from *n* = 11-12 brain slices for each bar; means ± SEM are shown. Data are representative of two independent experiments.

Abbreviations

Htt	Huntingtin protein
HD	Huntington’s disease
DAG	diacylglycerol
YFP	yellow fluorescent protein
CFP	cyan fluorescent protein